

RSC Advances



This is an *Accepted Manuscript*, which has been through the Royal Society of Chemistry peer review process and has been accepted for publication.

Accepted Manuscripts are published online shortly after acceptance, before technical editing, formatting and proof reading. Using this free service, authors can make their results available to the community, in citable form, before we publish the edited article. This *Accepted Manuscript* will be replaced by the edited, formatted and paginated article as soon as this is available.

You can find more information about *Accepted Manuscripts* in the [Information for Authors](#).

Please note that technical editing may introduce minor changes to the text and/or graphics, which may alter content. The journal's standard [Terms & Conditions](#) and the [Ethical guidelines](#) still apply. In no event shall the Royal Society of Chemistry be held responsible for any errors or omissions in this *Accepted Manuscript* or any consequences arising from the use of any information it contains.



Journal Name

COMMUNICATION

Hybrids of cobalt nanochains and polyvinylidene fluoride with enhanced microwave absorption performance

Received 00th January 20xx,
Accepted 00th January 20xx

Sh u-Qing Lv,^a Ya-Fei Pan,^b Pei-Bo Yang,^b and Guang-Sheng Wang*^b

DOI: 10.1039/x0xx00000x

www.rsc.org/

By using a simple wet chemical method and hot-molding procedure, a kind of flexible film based on binary cobalt nanochains/polyvinylidene fluoride (PVDF) hybrids have been successfully fabricated. Compared with pure metallic Co, the microwave absorption performance of binary hybrids exhibits obvious enhancement because of the synergistic effects occurred in components. The minimum reflection loss can reach -16.1 dB at 11.7 GHz, and the absorption bandwidth with a reflection loss below -10 dB is up to 10.4 GHz. The successful fabrication route offers an approach to design advanced microwave absorbers, which can be applied in commercial and military fields.

Introduction

With the extensive use of electromagnetic waves in the GHz frequency range used in electronic instruments in recent years, the materials of electromagnetic interference (EMI) shielding and attenuation have attracted much attention due to their significant role in preventing the electromagnetic pollution.¹⁻³ A high-performance microwave absorption material with strong absorption, wide absorption frequency, lightweight and high thermal stability, was considered as the ideal material which has practical applications in the fields of aerospace, automobile, and fast-growing new-generation miniaturized electronics.^{4,5} In the past decades, many efforts have been made to develop high-performance microwave absorption materials, and a variety of materials, such as ferrites, ceramics, metallic magnets, and their hybrids, have been successfully prepared and exhibited promising microwave absorption performance at GHz frequency range.⁶ In particular, lots of researchers have invested considerable effort in developing magnetic materials to use for microwave absorption, such as, Fe₃O₄ nanorings,^{7,8} Fe₃O₄/C nanorings,⁹ and rambutan-like Ni/MWCNT hybrids.¹⁰

As a candidate for microwave absorption, cobalt can attenuate EM waves efficiently, which is typical double-complex medium with dielectric loss and magnetic loss. Extensive studies have been conducted on the synthesis of metallic cobalt microwave absorbers with various special and complex nanostructures. For example, considering the impedance matching problem, hollow porous Co spheres, Copolypyrrole, Co-polystyrene, and Co/graphene, have been reported that all the materials can show the good microwave absorption performance.¹¹⁻¹⁴ In addition to designing those structures, concentrating on fabricating of one dimensional (1D) nanomaterials is also an alternative method to improve the microwave absorption performance. Permeability values of traditional microwave magnetic materials are small at GHz frequency range due to Snoek's limit. The large anisotropy of 1D nanomaterials may overcome the problem, and the intrinsic high frequency properties could be enlarged greatly compared the materials traditionally constrained by Snoek's limit.^{15,16} Until now, the advantages of 1D nanomaterials applied for microwave absorbers have been proved by some groups. Qiao et al.¹⁷ synthesized Ni nanowires which can attenuate approximately 90% of EM wave energy with 65 wt% filler content in GHz frequency range. Zhan et al.¹⁸ fabricated Fe nanochains by the chemical method, and obtained the minimum reflection loss of -20.4 dB for thickness of 2mm at 10.86 GHz.

We noticed that the general metallic cobalt and their nanocomposites used as the fillers in microwave absorbers have shortcomings of poor flexibility and high density which will restrict their wide applications as microwave absorbers. To solve these problems, we choose the polyvinylidene fluoride (PVDF) as a matrix for synthesizing the composites. Owing to the fact that the polymer possesses a high flexibility and permittivity, the PVDF is widely used as a matrix for polymeric composite materials with specific properties. Moreover, with the special chemical structure ($[-CH_2-CF_2-]_n$),^{19,20} the PVDF not only makes the composites be tailored as you want, but also may have the effects on enhancing the absorption abilities through the synergistic effect.

^a School of Civil Engineering, Northeast Dianli University, Jilin 132012, PR China.

^b Key Laboratory of Bio-Inspired Smart Interfacial Science and Technology of Ministry of Education, School of Chemistry and Environment, Beihang University, Beijing 100191, PR China. E-mail: wanggsh@buaa.edu.cn

*Electronic Supplementary Information (ESI) available: [details of any supplementary information available should be included here]. See DOI: 10.1039/x0xx00000x

To the best of our knowledge, research about involving the wave absorption properties of the cobalt nanochains/PVDF composites which utilize PVDF as the matrix has not been reported by other groups yet. In this paper, a simple wet chemical route was used to fabricate the nanochains and we combined them with flexible polymer PVDF firstly by a hot press method. Moreover, the wave absorption properties were investigated and the mechanism of enhanced wave absorption properties was also investigated in detail.

Experimental section

Commercially available reagents were analytical grade and used without further purification.

Preparation of nanochain-like cobalt products

The nanochain structure was synthesized using wet chemical method developed by Shi et al.²¹ The detailed synthetic procedure is as follows: 0.19 g $\text{CoCl}_2 \cdot 6\text{H}_2\text{O}$ and 0.5 g polyvinyl pyrrolidone (PVP, $M_w = 58000$) were dissolved in the 50 ml solvent ethylene glycol (EG) at room temperature by intensive stirring for 2 h and a homogenous transparent solution was obtained. Then 0.4 ml hydrazine monohydrate liquid (80%) was dropped to the mixture during the stirring process. And the solution turned turbid and pink, the stirring process lasted for 1 h after finishing the dropping. After that, the solution was heated to the boiling point of EG for refluxing ($\sim 197^\circ\text{C}$) by the heating jacket. After the mixture was refluxed for 1 hour, a dark precipitate was obtained. Then the product was washed with deionized water and ethanol several times. At last, the samples were obtained by centrifugation and dried at 60°C under vacuum.

Fabrication of Co nanochains/PVDF composite papers

The desired amount of PVDF was added in to the 30 ml of N,N -dimethylformamide (DMF) for 1h. Then, the cobalt nanochains were dispersed in the suspension under ultrasonication for another 1h. At last, the mixture was poured onto a glass plate to form a thin paper, and dried at 70°C for 1 day. The samples for testing were made by hot-pressing method to stack together at 200°C under 6 MPa.

Characterization

X-ray powder diffraction (D/MAX-1200, Rigaku Denki Co. Ltd, Japan) with Cu K α radiation at $\lambda=0.15406$ nm was used for the structural determination. Further microstructure analyses were performed using scanning electron microscopy (SEM, JSM-7500F) and transmission electron microscopy (TEM, JEOL-2100F). TEM samples were prepared by dispersing the powder products in alcohol by ultrasonic treatment, dropping the suspension onto a holey carbon film supported on a copper grid, and drying it in air. The lakeshore vibrating sample magnetometer (VSM, Riken Denshi Co. Ltd, Japan) was used to measure the magnetic properties of the samples at room temperature.

Microwave absorption performance measurement

The samples used for EM absorption measurement were pressed into a cylindrical shaped compact ($\Phi_{out}=7.00$ mm and $\Phi_{in}=3.04$ mm) by mixing the products with paraffin wax or PVDF in different mass

percentages. The EM parameters of the samples were measured by the transmission/reflection coaxial line method. And the values of complex permittivity and permeability were measured in the 2-18 GHz frequency range by an Agilent N5244a network analyzer.

Results and discussion

The representative morphology is shown in Fig. 1(a, b), which indicate that the samples consist of large quantities of ball chain-like structures. The 1D chains are made up of spherical nanoparticles, which display with the diameter about 500 nm. The Fig. 1c shows a TEM image of the single cobalt chain. It can be clearly seen that every cobalt sphere is connected by adjacent particles closely, which guarantees the materials can not break easily under the external action. Besides, the selected area electron diffraction (SAED) pattern (inset of Fig. 1c) corresponding to the circled area shows perfect single crystal nature of Co nanochains. The lattice fringes can be observed from a high-resolution TEM image in Fig. 1d. The neighboring distance is approximately 0.20 nm, which is relative to the (002) plane correctly.²² And the XRD pattern of nanochains, identified as hexagonal cobalt, is also shown in Fig. S1. More interestingly, one can see from Fig. 1e that the Co/PVDF film is easily bended repeatedly and shows magnetism to some extent. The film can also be cut into different shapes as you want. Thus, the flexible film has potential applications in special materials and devices. The Fig. S2 reveals the uniform dispersion of Co nanochains in polymer from the corresponding elemental maps of the Co, C, and F.

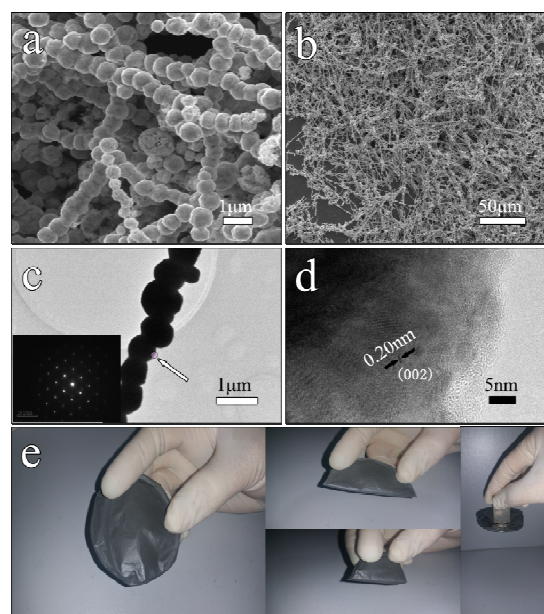


Figure 1. (a), (b) SEM image overviews of the as-prepared cobalt nanochains; (c) TEM image and SAED pattern (inset) of samples; (d) High resolution TEM image; (e) Digital photographs of the flexible and magnetic Co/PVDF paper.

Field dependent magnetization was measured at room temperature, and the result is plotted in Fig. 2. The saturation magnetization (M_s), remanent magnetization (M_r), and coercivity (H_c) of the products are 13.1 emu/g, 0.73 emu/g and 100.5 Oe, respectively. Compared with Co microspheres,²² the value of M_s becomes smaller owing to the presence of the residual PVP over the surface. On the other hand, the coercivity value of Co nanochains increase, which makes them possess larger magnetocrystalline anisotropic energy, meaning that is in favor of enhancement of microwave absorption.^{23, 24} In addition, the hysteresis loop of samples expresses typical ferromagnetic behavior.

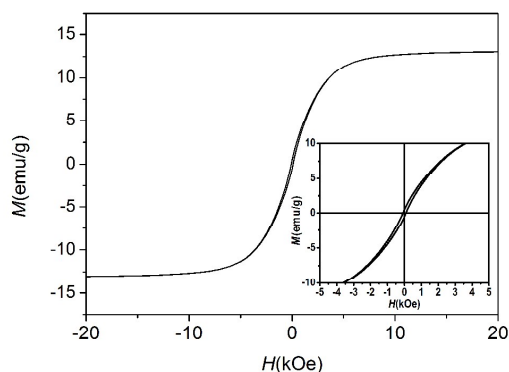


Figure 2. Magnetization hysteresis loop of the Co nanochains measured at room temperature.

Due to the 1D structure and the synergistic effects occurred in components, the samples may exhibit good microwave absorption properties. Therefore, various contents of samples mixed with paraffin wax or PVDF to prepare composites in a press process to measure microwave absorption performance. Based on the tested data of relative permittivity and permeability, the reflection loss (RL) values can be obtained by the following expression:²⁵

$$R = 20 \log \left| \frac{Z_{in} - 1}{Z_{in} + 1} \right| \quad (1)$$

where Z_{in} is the normalized input characteristic impedance, which can be expressed as:

$$Z_{in} = \sqrt{\frac{\mu_r}{\epsilon_r}} \tanh \left[j \left(\frac{2f\pi d}{c} \right) \sqrt{\mu_r \epsilon_r} \right] \quad (2)$$

where ϵ_r ($\epsilon_r = \epsilon' - j\epsilon''$) and μ_r ($\mu_r = \mu' - j\mu''$) are the complex permittivity and permeability of absorber; f is the frequency; d is the thickness of the absorber, and c is the velocity of light in free space.

Fig. 3a shows the theoretical reflection loss (RL) of composites 40 wt% Co/wax, 20 wt% Co/PVDF, 30 wt% Co/PVDF, 40 wt% Co/PVDF at a thickness of 2.5 mm. It shows that the RL of 40 wt% Co/PVDF is much higher than other hybrids. The minimum reflection loss of the composites reaches -16.1 dB at 11.7 GHz, the frequency bandwidth less than -10 dB is from 9.4 to 12.6 GHz. Fig. 3b shows the calculated theoretical reflection loss of Co/PVDF at various thickness (2-5 mm) with the filler loading of 40 wt%. It

indicates that the microwave absorption properties and the minimum RL corresponding to the maximum absorptions gradually appeared in different frequency can be tunable by controlling the thickness of the absorbers. And it worth noted that the materials attained a reflection loss of less than -10 dB in the frequency range from 7.6 to 18 GHz with an absorber thickness of 2.0-5.0 mm, which is over a half of the width between 2 and 18 GHz, confirming that this kind of composite is a broadband wave absorption material, which is quite beneficial to many electromagnetic shielding material designed to reduce electromagnetic waves over a wide frequency range. To demonstrate the microwave absorption properties more vividly, the three-dimensional presentation of reflection loss is also shown in Fig. 3c. We can find that the colour map of reflection loss reveals two minimum loss peaks gradually displayed with a larger thickness.

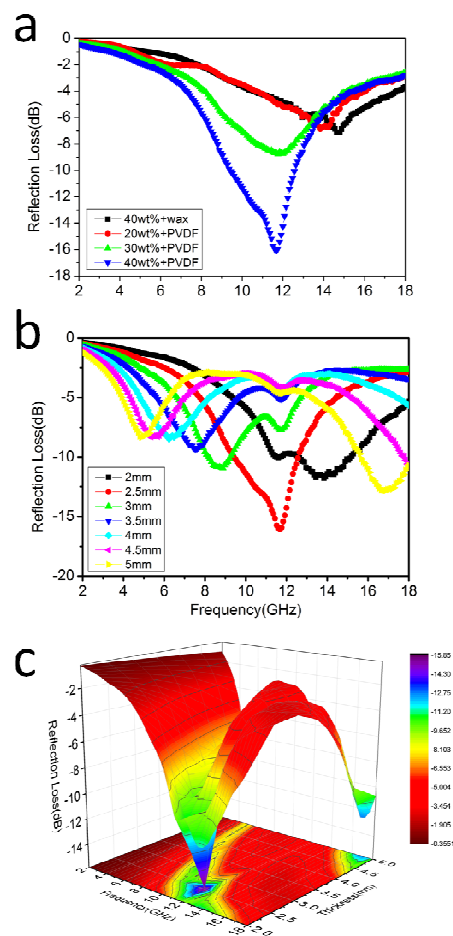


Figure 3. Reflection loss of (a) the products with a thickness of 2.5 mm in the range of 2-18 GHz; (b) the 40 wt% filler content of Co/PVDF composites with thickness 2-5 mm; (c) three-dimensional presentations of the reflection loss of the 40 wt% filler content of Co/PVDF composites.

Fig. 4(a-c) show the three-dimensional presentations of calculated reflection loss of various samples with different thickness in the range of 2-18 GHz. It can be observed that the absorption

performance of 40 wt% Co/wax hybrid is similar to 20 wt% Co/PVDF. That means that the similar absorption performance of Co/PVDF can be obtained with lower filler content, compared with Co/wax composites. And the Co/PVDF can exhibit a better test result than Co/wax at same loading contents, suggesting the PVDF matrix is important to enhancement of microwave absorption properties, and synergetic enhancement can happen between Co nanochains and PVDF. Furthermore, we can conclude that the more minimum reflection loss can reach with larger filler contents.

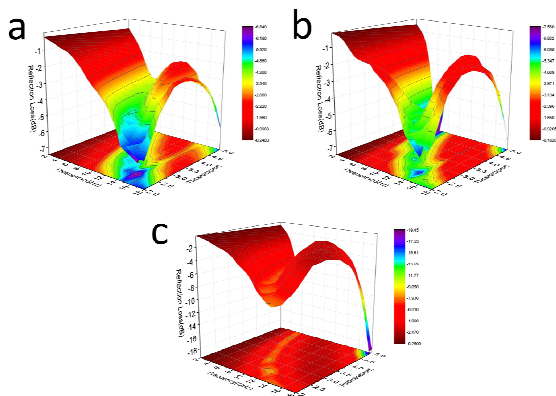


Figure 4. Three-dimensional presentations of the reflection loss of (a) Co/wax with a loading of 40 wt%; (b) Co/PVDF with a loading of 20 wt%; (c) Co/PVDF with a loading of 30 wt%.

To investigate the possible electromagnetic wave absorption mechanism of samples, the frequency dependence real permittivity and permeability, dielectric loss and magnetic loss are displayed in Fig. 5. The frequency dependence imaginary permittivity and permeability are also shown in Fig. S3. As we all know, the real permittivity and permeability are connected with the storage ability of electromagnetic energy, whereas the imaginary permittivity and permeability are linked with energy dissipation.²⁶ It can be seen that the values of ϵ' and dielectric loss ($\tan \delta = \epsilon''/\epsilon'$) for 40 wt% Co/PVDF hybrids is larger than others, indicating which bring about remarkable interface polarization. After combing with PVDF, the values of ϵ' and dielectric loss are also higher than Co/wax, suggesting that PVDF can influence the dielectric behaviors of the hybrids effectively. The maximum value of dielectric loss is 0.19 (11.7 GHz), which is in accordance with the reflection loss peak (shown in Fig. 3a). The values of μ' obvious reduce as the frequency increase, which could be attributed to the relaxation of magnetic moments procession instead of magnetic hysteresis, demonstrating the measuring frequency is higher than the relaxation frequency of the composite materials.²⁷ The values of magnetic loss maintain almost higher than 0.1 when combining with PVDF in all frequency region, implying the magnetic loss plays an important role for EM wave absorption.

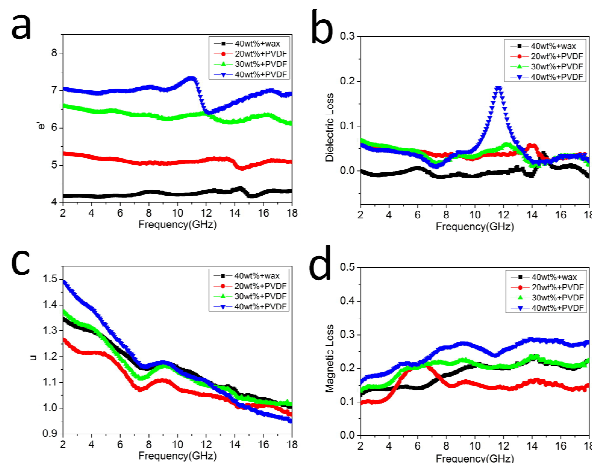


Figure 5. (a) Real part of complex permittivity; (b) dielectric loss; (c) real part of complex permeability and (d) magnetic loss of the products in the frequency range of 2-18 GHz.

According to the van der Zaag's research achievement,²⁸ the magnetic loss mainly derives from hysteresis, domain wall resonance, natural resonance, eddy current effect for magnetic materials. But, the hysteresis loss can be ignored in weak field, and domain wall resonance loss usually occurs at MHz frequency.^{29, 30} Therefore, the natural resonance and eddy current effect may be responsible for the attenuation of EM waves over 2-18 GHz frequency range. The natural resonance can be expressed in the following equation:³¹

$$2\pi f_r = rHa \quad (3)$$

$$Ha = 4|K_1|/3\mu_0 Ms \quad (4)$$

where r is the gyromagnetic ratio, Ha is the anisotropy energy, and $|K_1|$ is the anisotropy coefficient, Ms is the saturation magnetization. The resonance frequency depends on the effective anisotropy field, which is associated with coercivity value of the materials.^{32, 33} Just as the hysteresis loop curve shown in Fig. 2, there is a reversible rotational magnetization process when magnetic field are applied to Co nanocrystal, which means a relative high coercivity value exists. The reversible rotation of the magnetization vector is of benefit to improve permeability in the high frequency, which is also beneficial to EM wave absorption.³⁴ Aiming to research the influence of eddy current loss, $C_\sigma f$ curve for 40 wt% Co/PVDF composites is displayed in Fig. 6. The eddy current loss can be calculated by the following equation:

$$\mu'' \approx 2\pi\mu_0 (\mu')^2 \sigma \cdot d^2 f / 3 \quad (5)$$

where μ_0 ($H \cdot m^{-1}$) and σ ($S \cdot cm^{-1}$) are the electric permeability and the conductivity in vacuum, respectively. If the reflection loss is caused by eddy current loss effect, the values of C_0 ($C_0 = \mu''(\mu')^{-2} f^{-1}$) are constant when the frequency varies.³⁵ From Fig. 6, it can be

observed that the value of $C_{\sigma}f$ fluctuates in the 2-18 GHz frequency range, implying that the composites have no obvious eddy current effect for the microwave energy dissipation.

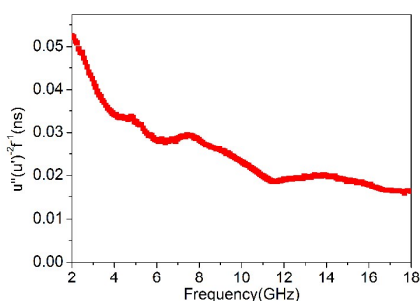


Figure 6. The $C_{\sigma}f$ curve of 40 wt% Co/PVDF composites.

We have analyzed the magnetic loss mainly originates from natural resonance in the above. In addition, the existence of interface between metallic Co and polymers gives rise to interfacial polarization, which depends on the conductivity and permittivity of the constituents of composites.^{3, 36, 37} This phenomenon appears in heterogeneous media due to the accumulation of charges at the interfaces and the formation of large dipoles on chains. The electronic dipole polarization also contributes to the synergistic effect because of increase of conductivity, caused by the additional coating of conductor Co on the polymer surface. A high concentration of Co in this composite creates considerable increase in the conductivity, which would result in strong dielectric loss according to the free-electron theory. And different phases would induce the electron wave packets that travel along these parts to cause electron interference loss.⁸ Moreover, when the incident microwaves act on the hybrids, they would be continuously reflected and refracted in the interspace, thus, multiple scattering and multiple loss are greatly carried out. Hence, we can conclude that the synergistic effects between Co nanochains and PVDF are caused by natural resonance, interfacial polarization, electronic dipole polarization and multiple scattering together, as shown in Fig. 7.

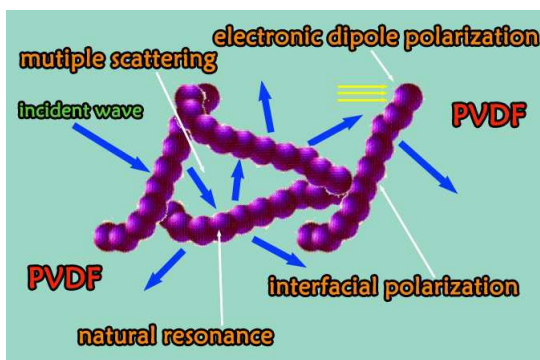


Figure 7. Schematic of the synergistic enhancement of microwave absorption performance between Co nanochains and PVDF.

Conclusions

We synthesized the ball chain-like Co nanostructures by a simple wet chemical method and Co/PVDF hybrids using the blending and hot-molding procedure. The composites exhibit an enhancement of microwave absorption performance in term of both the minimum reflection loss value and the absorption bandwidth over 2-18 GHz. The minimum reflection loss can reach -16.1 dB at 11.7 GHz, and the absorption bandwidth with a reflection loss below -10 dB is up to 10.4 GHz. The mechanism for enhancement of microwave absorption performance derived from the synergistic effect occurred in components, including electronic dipole polarization, interfacial polarization, natural resonance, and multiple scattering. It is believed that the Co nanochains/PVDF hybrids are good candidate for microwave absorption absorbers, which are promising for applications in military and commercial fields.

Acknowledgements

This project was supported by the National Natural Science Foundation of China (No. 51472012), and the Fundamental Research Funds for the Central Universities.

Notes and references

- X.-M. Meng, X.-J. Zhang, C. Lu, Y.-F. Pan and G.-S. Wang, *J. Mater. Chem. A*, 2014, **2**, 18725-18730.
- Y.-F. Pan, G.-S. Wang and Y.-H. Yue, *RSC Adv.*, 2015, **5**, 71718-71723.
- S. He, G.-S. Wang, C. Lu, J. Liu, B. Wen, H. Liu, L. Guo and M.-S. Cao, *J. Mater. Chem. A*, 2013, **1**, 4685-4692.
- Z. Liu, G. Bai, Y. Huang, F. Li, Y. Ma, T. Guo, X. He, X. Lin, H. Gao and Y. Chen, *J. Phys. Chem. C*, 2007, **111**, 13696-13700.
- V. K. Singh, A. Shukla, M. K. Patra, L. Saini, R. K. Jani, S. R. Vadera and N. Kumar, *Carbon*, 2012, **50**, 2202-2208.
- Y. Zhang, Y. Huang, T. Zhang, H. Chang, P. Xiao, H. Chen, Z. Huang and Y. Chen, *Adv. Mater.*, 2015, **27**, 2049-2053.
- Y. Liu, T. Cui, T. Wu, Y. Li and G. Tong, *Nanotechnology*, 2016, **27**, 165707.
- G. Tong, Y. Liu, T. Cui, Y. Li, Y. Zhao and J. Guan, *Appl. Phys. Lett.*, 2016, **108**, 072905.
- T. Wu, Y. Liu, X. Zeng, T. Cui, Y. Zhao, Y. Li and G. Tong, *ACS Appl. Mater. Inter.*, 2016, **8**, 7370-7380.
- G. Tong, F. Liu, W. Wu, F. Du and J. Guan, *J. Mater. Chem. A*, 2014, **2**, 7373-7382.
- C. He, S. Qiu, X. Wang, J. Liu, L. Luan, W. Liu, M. Itoh and K.-i. Machida, *J. Mater. Chem.*, 2012, **22**, 22160-22166.
- H. Wang, N. Ma, Z. Yan, L. Deng, J. He, Y. Hou, Y. Jiang and G. Yu, *Nanoscale*, 2015, **7**, 7189-7196.
- A. Ansari and M. J. Akhtar, *RSC Adv.*, 2016, **6**, 13846-13857.
- G. Pan, J. Zhu, S. Ma, G. Sun and X. Yang, *ACS Appl. Mater. Inter.*, 2013, **5**, 12716-12724.

15. G. Chai, D. Xue, X. Fan, X. Li and D. Guo, *Appl. Phys. Lett.*, 2008, **93**, 152516.
16. X. Liu, Y. Chen, X. Cui, M. Zeng, R. Yu and G.-S. Wang, *J. Mater. Chem. A*, 2015, **3**, 12197-12204.
17. L. Qiao, X. Han, B. Gao, J. Wang, F. Wen and F. Li, *J. Appl. Phys.*, 2009, **105**, 053911.
18. X. Zhan, H. Tang, Y. Du, A. Talbi, J. Zha and J. He, *RSC Adv.*, 2013, **3**, 15966-15970.
19. S. He, C. Lu, G.-S. Wang, J.-W. Wang, H.-Y. Guo and L. Guo, *ChemPlusChem*, 2014, **79**, 569-576.
20. G.-S. Wang, Y.-Y. Wu, X.-J. Zhang, Y. Li, L. Guo and M.-S. Cao, *J. Mater. Chem. A*, 2014, **2**, 8644-8651.
21. X.-L. Shi, M.-S. Cao, J. Yuan and X.-Y. Fang, *Appl. Phys. Lett.*, 2009, **95**, 163108.
22. Y. Zhang, F. Liang, N. Wang, L. Guo, L. He, C. Chen, Q. Zhang and Q. Zhong, *J. Nanosci. Nanotechnol.*, 2008, **8**, 2057-2061.
23. C. Wang, X. Han, X. Zhang, S. Hu, T. Zhang, J. Wang, Y. Du, X. Wang and P. Xu, *J. Phys. Chem.C*, 2010, **114**, 14826-14830.
24. S. Wen, Y. Liu, X. Zhao, J. Cheng and H. Li, *Powder Technol.*, 2014, **264**, 128-132.
25. M.-S. Cao, X.-L. Shi, X.-Y. Fang, H.-B. Jin, Z.-L. Hou, W. Zhou and Y.-J. Chen, *Appl. Phys. Lett.*, 2007, **91**, 203110.
26. W. Zhou, X. Hu, X. Bai, S. Zhou, C. Sun, J. Yan and P. Chen, *ACS Appl. Mater. Inter.*, 2011, **3**, 3839-3845.
27. Q. Liu, Q. Cao, H. Bi, C. Liang, K. Yuan, W. She, Y. Yang and R. Che, *Adv. Mater.*, 2016, **28**, 486-490.
28. P. J. van der Zaag, *J. Magn. Magn. Mater.*, 1999, **196**, 315-319.
29. Y. Du, W. Liu, R. Qiang, Y. Wang, X. Han, J. Ma and P. Xu, *ACS Appl. Mater. Inter.*, 2014, **6**, 12997-13006.
30. M. Wu, Y. D. Zhang, S. Hui, T. D. Xiao, S. Ge, W. A. Hines, J. I. Budnick and G. W. Taylor, *Appl. Phys. Lett.*, 2002, **80**, 4404.
31. C. Kittel, *Phys. Rev.*, 1948, **73**, 155-161.
32. Y.-J. Chen, P. Gao, R.-X. Wang, C.-L. Zhu, L.-J. Wang, M.-S. Cao and H.-B. Jin, *J. Phys. Chem.C*, 2009, **113**, 10061-10064.
33. Y.-J. Chen, G. Xiao, T.-S. Wang, Q.-Y. Ouyang, L.-H. Qi, Y. Ma, P. Gao, C.-L. Zhu, M.-S. Cao and H.-B. Jin, *J. Phys. Chem.C*, 2011, **115**, 13603-13608.
34. X. G. Liu, B. Li, D. Y. Geng, W. B. Cui, F. Yang, Z. G. Xie, D. J. Kang and Z. D. Zhang, *Carbon*, 2009, **47**, 470-474.
35. X.-J. Zhang, G.-S. Wang, W.-Q. Cao, Y.-Z. Wei, J.-F. Liang, L. Guo and M.-S. Cao, *ACS Appl. Mater. Inter.*, 2014, **6**, 7471-7478.
36. E. R. Cooper, C. D. Andrews, P. S. Wheatley, P. B. Webb, P. Wormald and R. E. Morris, *Nature*, 2004, **430**, 1012-1016.
37. J. K. Nelson and C. F. John, *Nanotechnology*, 2004, **15**, 586.

Graphical abstract

